A new method based on finite-difference time-domain scheme for computing the band structure of 2D photonic crystals

Juhong Zou (邹巨洪), Zheng Liang (梁 正), and Zongjun Shi (史宗君)

Institute of High Energy of Electronics, University of Electronic Science and Technology of China, Chengdu 610054

A finite-difference time-domain (FDTD) scheme in Cartesian coordinate system is developed to analyze the guided-wave properties of a class of two-dimensional (2D) photonic crystals formed by square or triangular arrays of metal posts. With the application of the periodic boundary condition, the computing domain can be restricted to a unit cell. A modified Yee's grid is introduced to calculate the dispersive characteristic in the case of triangular lattice. As examples, several classic structures are analyzed, numerical results are compared with the results from other methods, and the agreement is found to be very good. This method can also be extended to the three-dimensioned (3D) case.

OCIS codes: 000.4430, 310.2790.

Photonic crystals, typically built of periodic metallic or dielectric lattices, have shown tremendous potential applications both in physics and engineering communities. The absence of electromagnetic modes inside a photonic band gap (PBG) provides us an opportunity to shape and mold the flow of light. Two-dimensional (2D) photonic crystals have been used in many applications such as the feedback mirror in laser diodes[1], the fiber cladding[2], mode selective devices which can be used in high power microwave (HPM) devices[3,4], etc..

A variety of methods have been used to calculate the dispersive characteristic of the photonic crystal. For analysis of PBG cavities, finite-element codes such as HFSS can do a good job[5]. For analysis of the guided-wave properties in PBG structure, the plane wave expansion method[6], multiple-scattering theory[7,8] (Korringa-Kohn-Rostoker method), coordinate-space finite-difference method[9,10] have been used. Due to the convergence problem, the plane wave expansion method is applicable only to the lattices with the size of conductors much smaller than the lattice period.

Finite-difference time-domain (FDTD) is also a proper candidate to analyze the guided-wave properties of photonic crystal. To reduce the computation, periodic boundary condition was applied to restrict the computing domain to a unit cell[11]. Qiu and He presented a FDTD method[12], which uses a square mesh to calculate the dispersive characteristics of the photonic crystal and a nonorthogonal mesh in a nonorthogonal coordinate system in the case of triangular lattice.

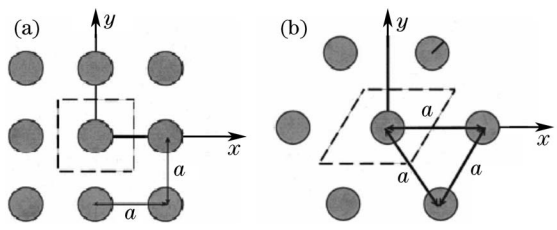

Fig. 1. Scheme of PBG structure representing (a) square lattice and (b) triangular lattice of perfectly conducting cylinders with radius of r and spacing a.

In this paper, we develop a method based on FDTD scheme in Cartesian coordinate system for both square lattice and triangular lattice, which is more simple and efficient than the nonorthogonal mesh[11]. A modified Yee's grid is introduced in the case of the triangular lattice. The numerical method is employed, numerical results are presented and the comparison is made between our results and the results from other methods.

The photonic crystal formed by square or triangular arrays of metal posts is considered here, namely the square lattice (Fig. 1(a)) and the triangular lattice (Fig. 1(b)), for these kinds of structures are in considerable interest recently[3,4,6,9,10,12].

Since the structure of the photonic crystal is periodic, the field should satisfy the Bloch theory so that

$$E(\mathbf{r}) = E(\mathbf{r})e^{-j\mathbf{k}\cdot\mathbf{r}}, H(\mathbf{r}) = H(\mathbf{r})e^{-j\mathbf{k}\cdot\mathbf{r}}, \tag{1}$$

where $E(\mathbf{r}), H(\mathbf{r})$ are periodic functions in space, and satisfy

$$E(\mathbf{r}+\mathbf{L}) = E(\mathbf{r}), H(\mathbf{r}+\mathbf{L}) = H(\mathbf{r}), \tag{2}$$

where $\mathbf{L}$ is the lattice vector. Since the system is homogeneous along the z-axis, we can set $k_z = 0$, which obviously dose not affect the generality of the results.

Substitute (1) into Maxwell's two curl equations, we get

$$\begin{aligned}
\mu\frac{\partial H_x}{\partial t} &= \frac{\partial E_y}{\partial z} - \frac{\partial E_z}{\partial y} + jk_y E_z,\\
\mu\frac{\partial H_y}{\partial t} &= \frac{\partial E_z}{\partial x} - \frac{\partial E_x}{\partial z} - jk_x E_z,\\
\mu\frac{\partial H_z}{\partial t} &= \frac{\partial E_x}{\partial y} - \frac{\partial E_y}{\partial x} - jk_y E_x + jk_x E_y,\\
\varepsilon\frac{\partial E_x}{\partial t} &= \frac{\partial H_z}{\partial y} - \frac{\partial H_y}{\partial z} - jk_y H_z,\\
\varepsilon\frac{\partial E_y}{\partial t} &= \frac{\partial H_x}{\partial z} - \frac{\partial H_z}{\partial x} + jk_x H_z,\\
\varepsilon\frac{\partial E_z}{\partial t} &= \frac{\partial H_y}{\partial x} - \frac{\partial H_x}{\partial y} - jk_x H_y + jk_y H_x.
\end{aligned} \tag{3}$$

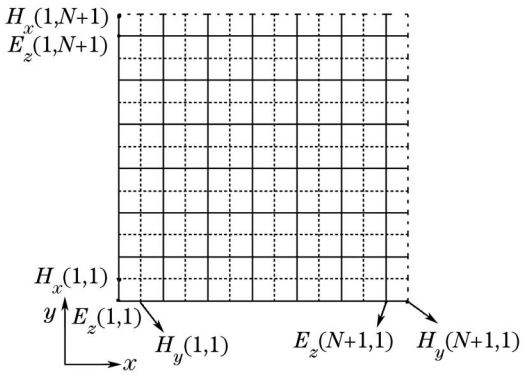

Fig. 2. Grid in a period for square lattice.

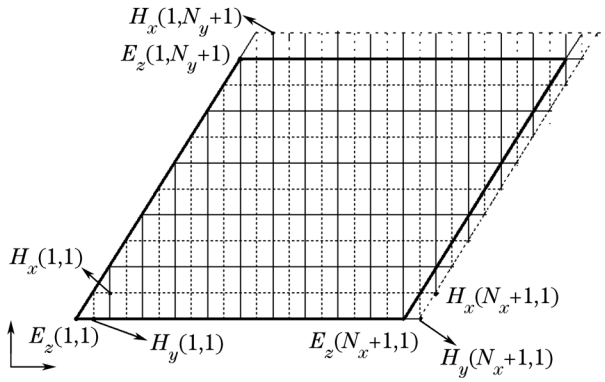

Fig. 3. Grid in a period for triangular lattice.

Considering TM modes first, in the case of square lattice, we discretize the entire period with $N \times N$ mesh shown in Fig. 2. This is a standard Yee's grid. To apply the period condition shown in Eq. 2, electric boundary is located in one side (solid line) and the other side is set to be magnetic boundary (dashed line).

For triangular lattice, we slightly modify the standard Yee's grid to discretize one period with a $N_x \times N_y$ mesh (Fig. 3), in which we take $\Delta y/\Delta x = \tan(\alpha)$, and denote each grid point by

$$(i,j) = (i\Delta x, j\Delta y). \tag{4}$$

The discretization of Eq. 3 becomes

$$\begin{aligned}
\varepsilon\frac{E_z^{n+1}(i,j)-E_z^n(i,j)}{\Delta t} &= \frac{H_y^{n+1/2}(i,j)-H_y^{1/2}(i-1,j)}{\Delta x} \\
&-\frac{H_x^{n+1/2}(i-1,j)-H_x^{n+1/2}(i,j-1)}{\Delta y} \\
&-jk_x\frac{H_y^{n+1/2}(i,j)+H_y^{1/2}(i-1,j)}{2} \\
&+jk_y\frac{H_x^{n+1/2}(i-1,j)+H_x^{n+1/2}(i,j-1)}{2}, \\
\mu\frac{H_x^{n+1/2}(i,j)-H_x^{n-1/2}(i,j)}{\Delta t} &= \\
&-\frac{E_z^n(i,j+1)-E_z^n(i+1,j)}{\Delta y} \\
&+jk_y\frac{E_z^n(i,j+1)+E_z^n(i+1,j)}{2}, \\
\mu\frac{H_y^{n+1/2}(i,j)-H_y^{n-1/2}(i,j)}{\Delta t} &= \frac{E_z^n(i+1,j)-E_z^n(i,j)}{\Delta x} \\
&-jk_x\frac{E_z^n(i+1,j)+E_z^n(i,j)}{2}.
\end{aligned} \tag{5}$$

To descretize the periodic boundary condition, we can treat it in the same way as in square lattice. And in the case of TE modes, we can treat it in a similar way.

So far, with the application of periodic boundary condition, we can restrict the possible values of $k_\perp$ to the irreducible Birllouin zones of the reciprocal lattices shown in Fig. 4.

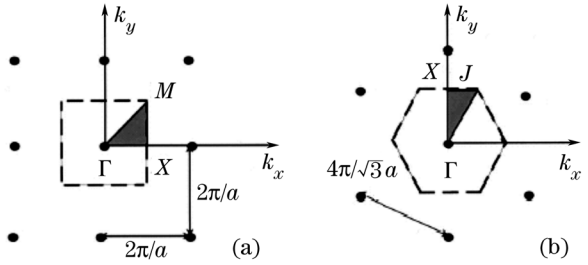

Fig. 4. Reciprocal lattices and Brillouin zones for (a) square lattice and (b) triangular lattice (irreducible Brillouin zones for each type of lattice are shaded).

When begin interative, we preset the value of $k_\perp$, place the Gaussian impulse at one point as excitation source, and another point is chosen to be the sense point to record the field information every time step. After the FDTD scheme, we need to transform the calculated field information from the time domain to the frequency domain by Fourier transform. The peaks of the spectral distribution correspond to the location of the eigen frequencies for the given $k_\perp$.

Now we present our FDTD numerical results and compare them with the results from other methods. In all the computation, the total number of time steps is 5000 with each time step $\Delta t = 1/(2c)$.

In the case of square lattice, choose $N = 40$, the radius of the metal posts is set to be $R = 0.2a$, where a is the lattice constant. Figure 5(a) shows the dispersion characteristics for several lowest TM modes as the wave vector changes from Γ point in the Birllouin zone shown in Fig. 4(a) to X, and then to M. There is a global band gap between the first and the second TM modes. Figure 5 (b) shows the dispersion characteristics for several lowest TE modes as the wave vector changes from Γ point in the Birllouin zone shown in Fig. 4(a) to X, and then to M. The first and second TE modes are intersecting and there is no global band gap.

In the case of triangular lattice ($\alpha = 60°$), choose $N_x = 40, N_y = 80$, the radius of the metal posts is set to be $R = 0.2a$, where a is the lattice constant. Figure 6(a) shows the dispersion characteristics for several lowest TM modes as the wave vector changes from

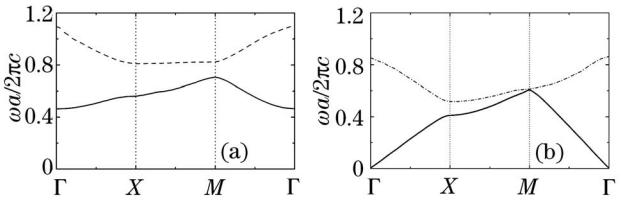

Fig. 5. Plots of the several lowest normalized eigenmodes versus the wave vector $k_\perp$ for TM (a) and TE modes (b) as $k_\perp$ varies from Γ point in the Birllouin zone shown in Fig. 4(a) to X, and to M for square lattice.

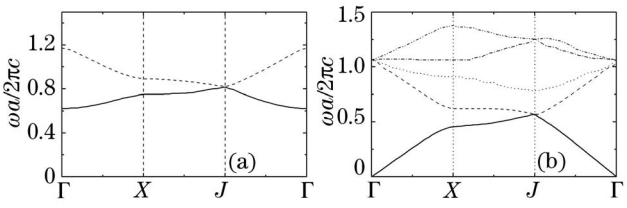

Fig. 6. Plots of the several lowest normalized eigenmodes versus the wave vector $k_\perp$ for TM (a) and TE modes (b) as $k_\perp$ varies from Γ point in the Birllouin zone shown in Fig. 4(b) to X, and to J for triangular lattice.

Γ point in the Birllouin zone shown in Fig. 4(b) to X, and then to J. Figure 6(b) shows the dispersion characteristics for several lowest TE modes as the wave vector changes from Γ point in the Birllouin zone shown in Fig. 4(b) to X, and then to J. There is no global band gap between the first and the second TM or TE modes.

All the results presented here are compared with the results from coordinate-space, finite-difference method[10], the deviation between them is less than 1%.

In conclusion, an efficient method based on FDTD scheme is presented to analyze the guided-wave properties of 2D photonic crystal. In the case of triangular lattice, we introduce a modified Yee's grid to simplify the compution, so that both square lattice and triangular lattice cases can be solved in Cartesian coordinate system. Results show that our code can be used to quickly and accurately get the guided-wave properties of 2D photonic crystal. Although here we only present the results of photonic crystal formed by arrays of metal posts, it can also analyze the case of dielectric inclusions. Besides, this method can be extended to 3D case. It can also be used to analyze the guided-wave properties of slow wave structure (SWS) in HPM devices, and the scatter problem in gratings.

J. Zou's e-mail address is feeless@sina.com.

References

1. D. L. Bullock, C. Shih, and R. S. Margulies, J. Opt. Soc. Am. B **10,** 399 (1993).
2. J. C. Knight, T. A. Birks, P. St. J. Russell, and D. M. Atkin, Opt. Lett. **21,** 1547 (1996).
3. J. R. Sirigiri, K. E. Kreischer, J. Machuzak, I. Mastovsky, M. A. Shapiro, and R. J. Temkin, Phys. Rew. Lett. **86,** 5628 (2001).
4. M. A. Shapiro, W. J. Brown, I. Mastovsky, Phys. Rev. Special Topics: Accelerators and Beams **4,** 042001 (2001).
5. Ansoft High Frequency Structure Simulator – User's Manual, Ansoft Corp. (1999).
6. T. Suzuki and P. K. L. Yu, Phys. Rev. B **57,** 2229 (1998).
7. X. Wang, X. G. Zhang, Q. Yu, and B. N. Economon, Phys. Re. B **47,** 4161(1993)
8. K. M. Leung and Y. Qiu, Phys. Rev. B **48,** 7767 (1993)
9. D. R. Smith, S. Schultz, and N. Kroll, Appl. Phys. Lett. **65,** 645 (1994).
10. E. I. Smimova, C. Chen, and M. A. Shapiro, J. Appl. Phys. **91,** 960 (2002).
11. A. C. Cangellaris, M. Gribbons, and G. Sohos, IEEE Microwave and Guide Wave Letters **3,** 375 (1993).
12. M. Q and S. He, J. Appl. Phys. **87,** 8268 (2000).